

INVESTIGATION OF THE SUPERSONIC FLOW PAST A WEDGE-SHAPED GEOMETRY USING PRESSURE SENSITIVE PAINTS TECHNIQUE

Jindřich Hála, David Šimurda, Jan Lepičovský, Martin Luxa

Institute of Thermomechanics of the Czech Academy of Sciences, Prague, Czech Republic

ABSTRACT

This study aims to present results of an investigation of the supersonic flow past a wedge-shaped geometry using the pressure sensitive paints technique (PSP). The wedge-shaped geometry was chosen as a canonical case for the investigation of the supersonic flow involving shock waves and strong expansion making it a convenient case to build a first practical experience with this technique, further intended for use in the investigation of linear blade cascades in high speed laboratory of the Institute of Thermomechanics of the Academy of Sciences of the Czech Republic. The tests on the wedge-shaped geometry were complemented with the numerical simulations and static pressure taps measurements. The resulting static pressure distribution obtained using the PSP on the wedge-shaped model revealed all main flow structures including positions of the separation and reattachment shocks providing a good picture of the whole flow field.

NOMENCLATURE

$C_{1,2,3}$	(1)	PSP calibration constants
I	(1)	red light intensity
M_1	(1)	inlet Mach number
M_{is}	(1)	isentropic Mach number
p	(Pa)	pressure
p_{01}	(Pa)	inlet total pressure
x	(mm)	span-wise coordinate
τ_w	(Pa)	wall shear stress
γ	(1)	heat capacity ratio

Subscripts

is	isentropic
ref	reference (no-flow conditions)

INTRODUCTION

Three dimensional effects are of significant concern in linear blade cascades research as the corner flow structures significantly affect the axial density velocity ratio (AVDR)[1][2], an important parameter in compressor cascades investigation. Suction slots or perforated walls can be used to control the corner flow structures and thus the AVDR. From the practical point of view, it is convenient to have a technique capable of exposing the extent of three dimensional effects during the

course of measuring campaign to allow for adequate setting of the suction. The pressure sensitive paints technique (PSP) seems to offer this and at the same time provide valuable data on the flow structures on the surface being investigated.

The present investigation was performed for an inlet Mach number $M_1 \approx 1.9$ and the wedge-shaped model was instrumented with multiple pressure taps to provide the static pressure data for an in-situ calibration of the PSP according to [3]. The resulting static pressure distribution well corresponds with the numerical simulations and capture the main flow features. The paper includes detailed description of the flow field and the comparison of the measurements with numerical simulation.

EXPERIMENTAL SETUP

The geometry of the wedge-shaped model consists of straight lower wall and the inclined upper wall with the length of 50 mm and the apex angle of 15° followed by straight wall. The total length of the model is 280 mm and width 160 mm (Figure 1).

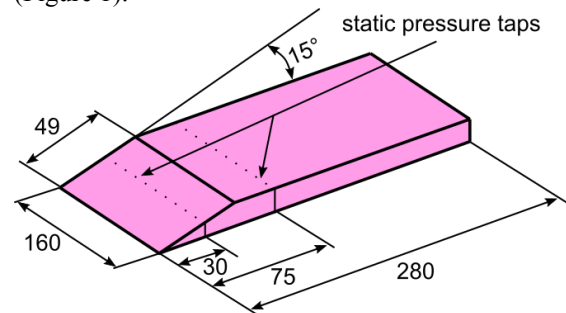


Figure 1. The isometric view of the wedge-shaped model with the main dimensions

The model was instrumented using static pressure taps located on the upper side located in two rows across the model width. One row was located on the inclined ramp 30 mm downstream the leading edge and the second one on the straight part of the upper wall in the distance of 75 mm from the leading edge. In total 18 pressure taps were located on the model surface. Besides the static pressure taps on the surface of the model, there was also a number of static pressure taps on the sidewall surface and in the settling chamber.

Further, the Prandtl probe inside the inlet part of the wind tunnel was also used.

The experiments were carried out in the dried air breathing in-draft type high-speed wind tunnel of the Institute of Thermomechanics of the Czech Academy of Sciences in Nový Knín (Figure 2). The inlet flow parameters were measured by a Prandtl probe and static pressure taps on the side-wall in front of the model. All measurements were performed for zero incidence angles.

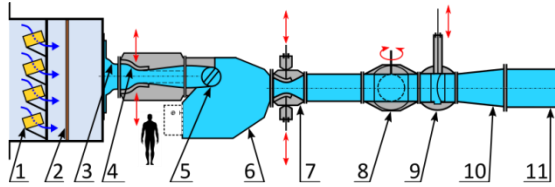


Figure 2. Scheme of the intermittent in-draft type high-speed wind tunnel: 1–silica gel dryer, 2–filters, 3–entrance nozzle, 4–inlet nozzle, 5–rotatable test section, 6–settling chamber, 7–control nozzle, 8–quick acting ball valve, 9–safety valve, 10–diffuser, 11–main duct

To obtain clear view necessary for the PSP technique, the model was mounted between two plexi-glass windows forming sidewalls of the test section. The schematic view of the test section with the wedge-shaped model inside is shown in Figure 3 and the actual view of the test section during the measurements in Figure 4.

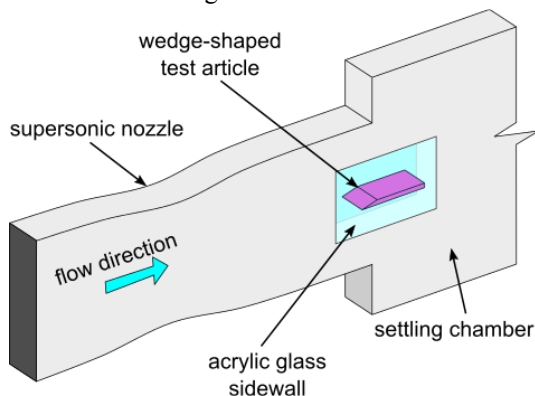


Figure 3. Schematic depiction of the wind tunnel test section with the wedge-shaped model inside

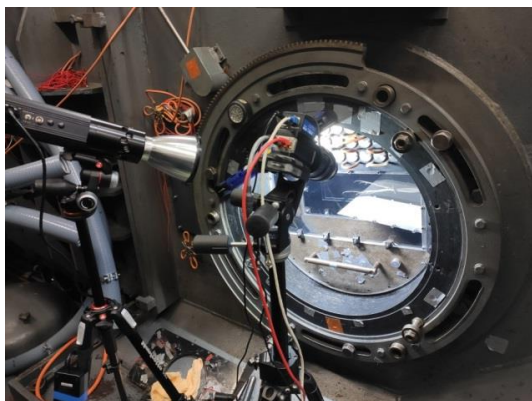


Figure 4. Actual view of the measured model in the wind tunnel test section

NUMERICAL SIMULATION

The problem was numerically modelled in 3D using the system of time-averaged Navier-Stokes equations for compressible flows. Since the flow medium is a dry air, the equation of state of an ideal gas was considered. The Reynolds stress tensor and the turbulent thermal diffusivity were computed using the $k-\omega$ SST turbulence model. The inviscid fluxes were approximated using the Advection Upstream Splitting Method (AUSM) upwind scheme with linear reconstruction. The steady state solution was obtained using the density-based implicit solver in Ansys Fluent commercial code employing second order accuracy upwind schemes in space.

The computational grid consisted of approximately $5 \cdot 10^6$ hexahedral cells. The domain was symmetric in the span-wise direction; therefore a symmetry boundary condition was used in the midspan plane. Walls were treated as no-slip and adiabatic. At the inlet, the total pressure profile measured in the wind tunnel was prescribed to account for boundary layer development inside the entrance part. Other inlet boundary conditions including static pressure corresponding to desired inlet Mach number M_1 were as follows:

Total temperature	$T_0 = 300 \text{ K}$
constant turbulence intensity	$Tu = 2\%$
constant turbulent viscosity ratio	$\mu_t/\mu = 10$
static pressure	$p = 15.1 \text{ kPa}$

PSP CALIBRATION

Calibration of the PSP was performed in-situ for each measurement run using a number of static pressure taps on the model surface. Then the calibration consists of finding calibration constants C_1 , C_2 and C_3 for the following calibration relation [3]

$$\frac{p}{p_{ref}} = C_1 + C_2 \frac{I_{ref}}{I} + C_3 \left(\frac{I_{ref}}{I} \right)^2 \quad (1)$$

where I and I_{ref} is the value of emitted red light intensity during the measurement and reference red light intensity for no-flow conditions, respectively. Similarly p and p_{ref} is the value of the static pressure measured using static pressure taps for flow and no-flow conditions, respectively. The calibration constants were computed using an optimization algorithm minimizing the objective function in the least square sense. An example of the calibration curve for one of the measuring runs can be seen in Figure 5.

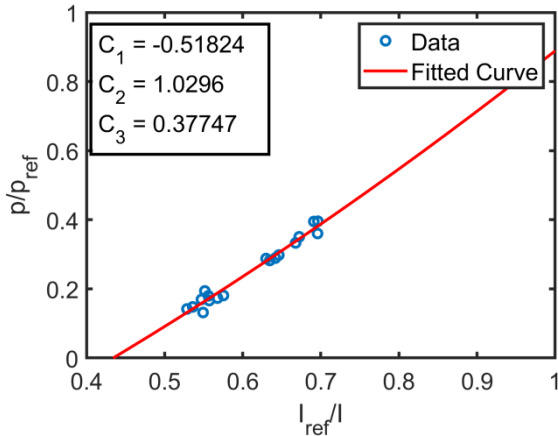


Figure 5. An example of the calibration curve for one of the measurement runs

RESULTS AND DISCUSSION

The interferogram in Figure 6 clearly shows the most significant flow features in the investigated flow-field consisting of the oblique shockwave (solid red line) generated on the wedge leading edge and the expansion fan (dashed green line). Knowing the static pressure at one point on the wedge surface, it is relatively straightforward to evaluate the pressure distribution over the wedge surface from the interferogram. However, such evaluation is distorted due to presence of density variations within the boundary layer on the test section walls [4]. It is because the light ray passing through the test section integrates all refraction index changes including those in boundary layers and in secondary flow structures into a single resulting value. These effects are inevitable in linear cascade research, thus any method capable to quantify their extent is important.

The static pressure distribution measured

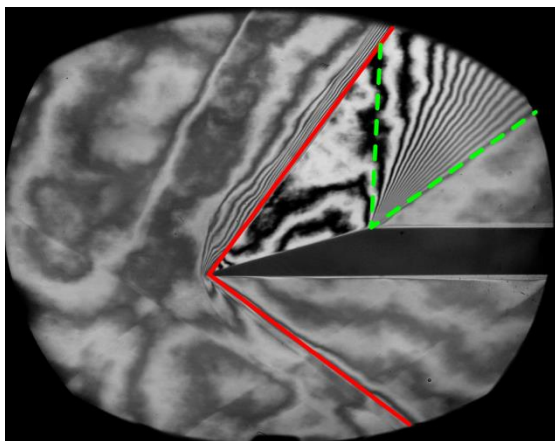


Figure 6. Interferogram of the flow past the wedge shaped geometry for the inlet Mach number $M_1 \approx 1.9$

using the PSP over the model together with the CFD simulation results can be seen in Figure 7. It is evident that the flow field is far from uniform in the span-wise direction. On the wedge ramp

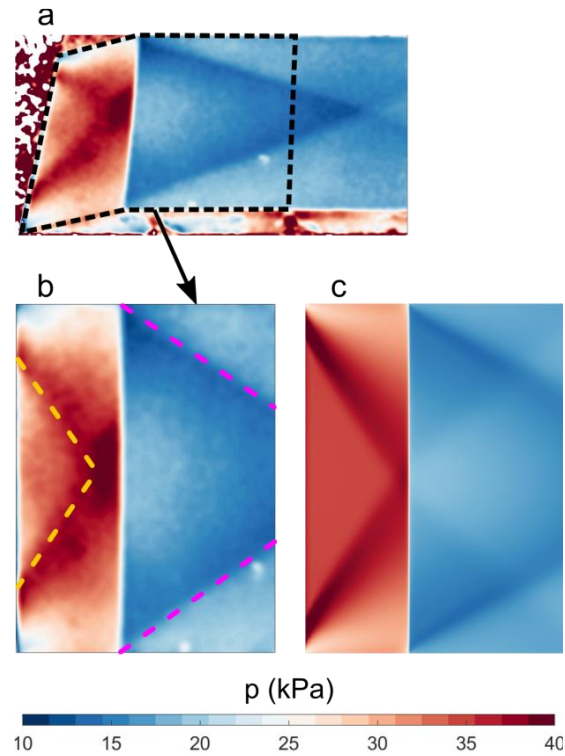


Figure 7. Static pressure contours measured using the PSP in the view as taken by a camera (a) and the view corrected for perspective (b) compared with the CFD computation (c)

surface we can observe traces of the shockwaves generated by the leading edge shockwave interaction with the boundary layers on the side walls (yellow dashed line in Figure 7b). This interaction is most likely accompanied with local flow separation as suggested by the computed wall-shear stress distribution on the sidewall surface that can be seen in Figure 8.

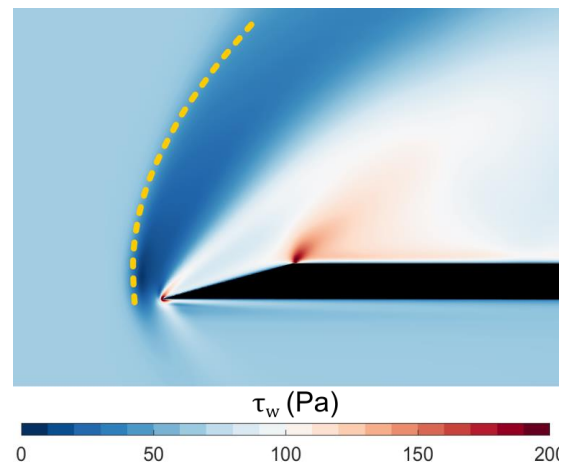


Figure 8. Wall shear stress contours computed using CFD with yellow dashed line marking the approximate position of the limiting streamline

Another shockwaves then stem from the locations of the joints of the end of the ramp with sidewalls (purple dashed line in Figure 7b). These waves are caused due to the sudden expansion in which the

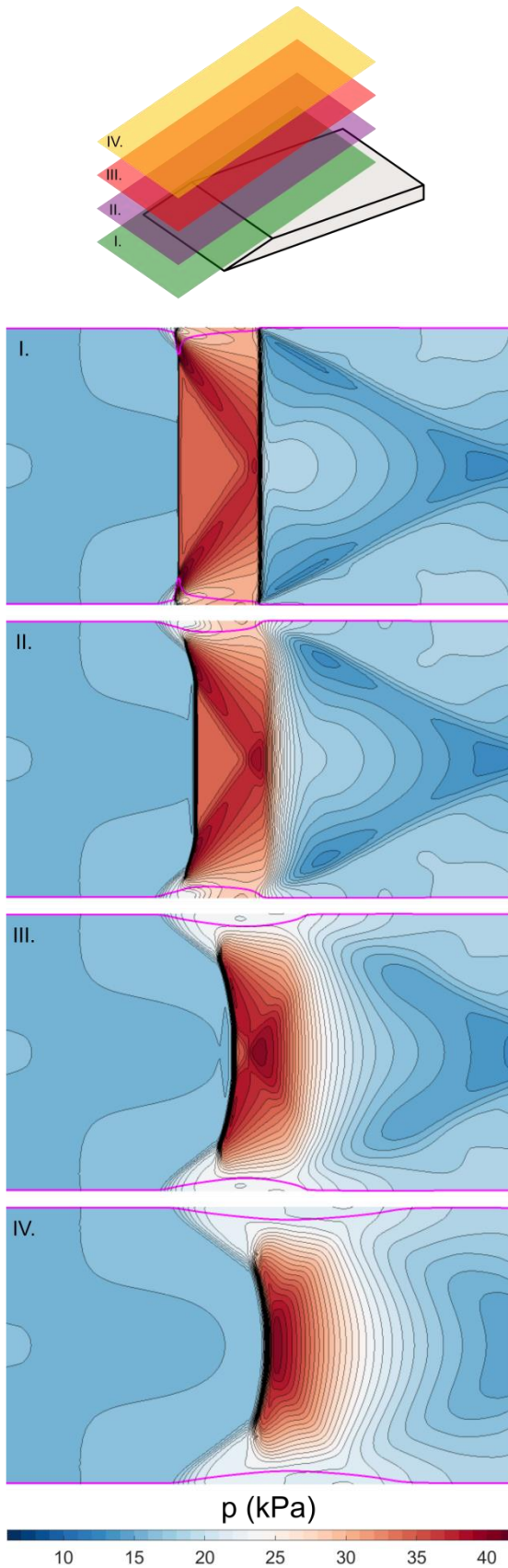


Figure 9 Computed pressure contours in planes parallel to the wedge ramp with marked sonic lines (solid purple lines)

boundary layer shrinks. There, the supersonic flow must follow the change in flow direction, which always produces shockwaves.

Computed pressure contours in four planes parallel to the wedge ramp in Figure 9. Computed pressure contours in planes parallel to the wedge ramp with marked sonic lines (solid purple lines) well demonstrate three dimensional character of the flow field. It can be seen that with increasing distance from the surface the subsonic area is getting bigger and the leading edge shockwave is getting more bulged with larger lambda splitting (cuts II, III and IV). Cut IV then shows the limiting case when the shockwave starts to interact with the expansion region caused by the end of the wedge ramp. The shockwave structures might from this point of view resemble the normal shockwave – boundary layer interaction, however, the shockwave is oblique with supersonic flow downstream even though it appears to be perpendicular to the side walls in cuts in Figure 9. An extent of the subsonic region on the sidewall can be seen in Figure 10, which shows the sidewall static pressure distribution measured using the PSP compared to CFD simulation. It can be seen that the region of increased static pressure reaches significantly upstream the location of the shock wave as pictured on the interferogram in Figure 6.

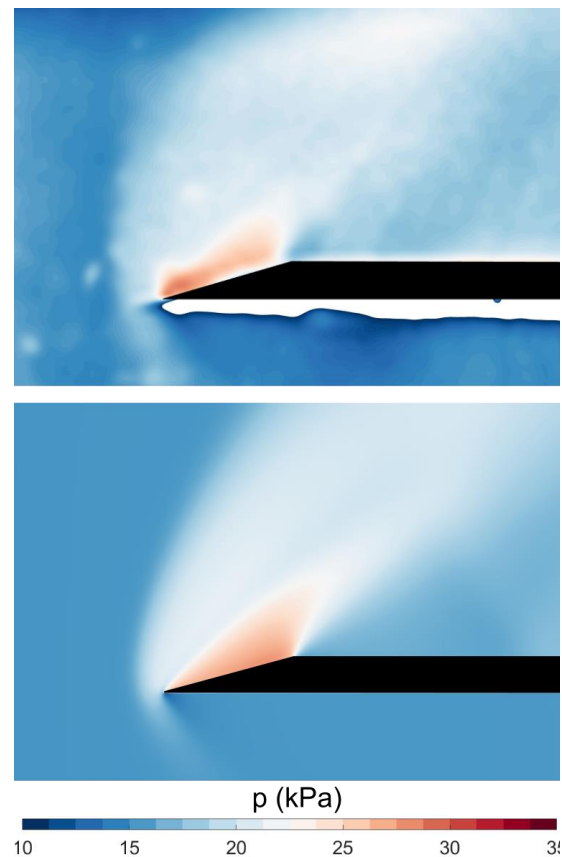


Figure 10. Static pressure contours on the sidewall. PSP (upper) and CFD (bottom)

A final comparison was made in terms of an isentropic Mach number distribution over the model surface since the isentropic Mach number defined as

$$M_{is} = \sqrt{\frac{2}{\gamma - 1} \left[\left(\frac{p}{p_{01}} \right)^{\frac{1-\gamma}{\gamma}} - 1 \right]} \quad (2)$$

is a common way of quantitative analysis of interferograms. The comparison was made to isentropic Mach number calculated from pressure distribution obtained from the PSP images in two manners. In the first one, the static pressure distribution in the mid-span was used while in the other one the resulting value on the model surface was calculated by integrating all values in the span-wise direction for given x (cord-wise) coordinate to mimic interferogram which integrates all changes across the flow field. The resulting graph is in Figure 11. It is evident that the actual mid-span distribution evaluated from PSP is substantially different from the one obtained using interferometry. At the same time the interferometry values and values obtained from the PSP integrated in span-wise direction correspond well.

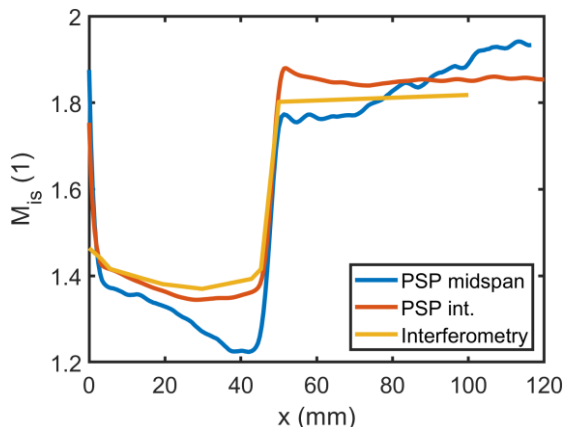


Figure 11. Comparison of the isentropic Mach number distributions over the model surface evaluated using interferometry and PSP

CONCLUSIONS

The paper describes the measurement of the supersonic flow around the wedge shaped geometry intended as a test case for measurement using the pressure sensitive paints in High speed laboratory of the Institute of Thermomechanics of the Czech academy of Sciences. The obtained results compared to numerical simulations proved this method promising for future deployment in linear blade measurements to help assess measurements and identify significant flow features. The only identified drawback was the sensitivity of the paint to grease contamination resulting in white spots visible in Figure 7 and Figure 10. For that reason, it is necessary to handle

the painted models very carefully which is not always easy in harsh wind tunnel environment.

The results have shown significant difference between mid-span isentropic Mach number distribution measured using PSP and that evaluated from interferogram due to three dimensional effects. However, all the tests were made without the boundary layer suction that might at least mitigate this effect.

Further research will be focused on the use of PSP together with borescope to obtain optical access to less accessible locations during the linear cascade measurements.

ACKNOWLEDGMENTS

This research was supported by the Czech Science Foundation (GACR) under grant no. 20-11537S. Institutional support RVO: 61388998 of the Institute of Thermomechanics of the Czech Academy of Sciences is also acknowledged.

REFERENCES

- [1] Song, B., Ng, W. F., (2007). The role of AVDR in linear cascade testing. *Hangkong Dongli Xuebao/Journal of Aerospace Power*. 22. 933-944.
- [2] Choi J., Simurda D., Song J., Luxa M., Lee S., Hala J., Lepicovsky J., Radnic T., Seo J. Development of loss correlation and tool validation at transonic condition based on cascade test, (2021), DOI: 10.1115/GT2021-01771.
- [3] Liu T, Sullivan JP (2005) Pressure and temperature sensitive paints. Springer, Berlin. <https://doi.org/10.1007/b137841>. ISBN 978-3-540-26644-0
- [4] Lepicovsky J., Luxa M., Simurda D., Effects of Flow Distortion on Clarity of Interferometer Data, (2020), DOI: 10.1115/GT2020-14378